257

Finite Elements in Fluids—Volume 6
Edited by R. H. Gallagher, G. F. Carey, J. T. Oden, and O. C. Zienkiewicz

Chapter 15

An Adaptive p-Version Finite Element Method for Transient Flow Problems with Moving Boundaries

L. Demkowicz, J. T. Oden, and T. Strouboulis

15.1 INTRODUCTION

We present in this paper a review of some preliminary results on the development of self-adaptive finite element methods for use in the study of transient two-dimensional flow problems in domains with moving boundaries. This study focuses on the so-called p-version of the finite element method, in which the degree p of the local polynomial shape functions is increased to enrich the quality of the approximation while the mesh size is kept fixed.

Our enrichment strategy is based on the calculation of reliable a posteriori error estimates over each element at the end of each time-step. These estimates are based on the assumption that the mesh size h is sufficiently small; thus the quality of these estimates improves with some refinement of the mesh. These estimates allow us to compute error indicators for each element at each time-step, and to compare the local element indicator with the total indicator for the whole mesh. When the local error indicator reaches a preassigned percent of the total, the local polynomial degree p is increased; conversely, when this local error is less than the critical percentage, our algorithm provides for the reduction in p so as to reduce the computational effort.

So as to provide for time-dependent moving boundaries, we develop a space–time variational formulation of the flow problem and corresponding space–time finite elements. A more detailed account of the methods described here is given in Demkowicz *et al.* (1984).

15.2 VARIATIONAL PRINCIPLES FOR FLOW PROBLEMS WITH MOVING BOUNDARIES

In order to incorporate the effects of a time-varying boundary on which time-dependent conditions are imposed into the formulation of flow problems, it is convenient to develop space–time variational statements of such problems in which the time-variable is integrated over a fixed interval $[0, T]$.

In the following we will use the following notation:

- Ω_t the spatial domain at time $t, t \in [0, T]$, an open bounded domain in $\mathbb{R}^2$ continuously dependent on t;
- $\partial\Omega_t$ the boundary of Ω_t consisting of two disjoint parts Γ_t^v and Γ_t^T where the kinematic and traction boundary conditions are prescribed respectively;
- D the space–time domain, $D = \bigcup_{0<t<T} \Omega_t$.

In the present study, we assume for simplicity that the 'moving portion' Γ_t^M of the boundary $\partial\Omega_t$ is always contained in Γ_t^v. An illustration of such a time-varying domain is given Figure 15.1.

The flow of an incompressible viscous fluid through a time-dependent domain is characterized by the transient Navier–Stokes equation with appropriate

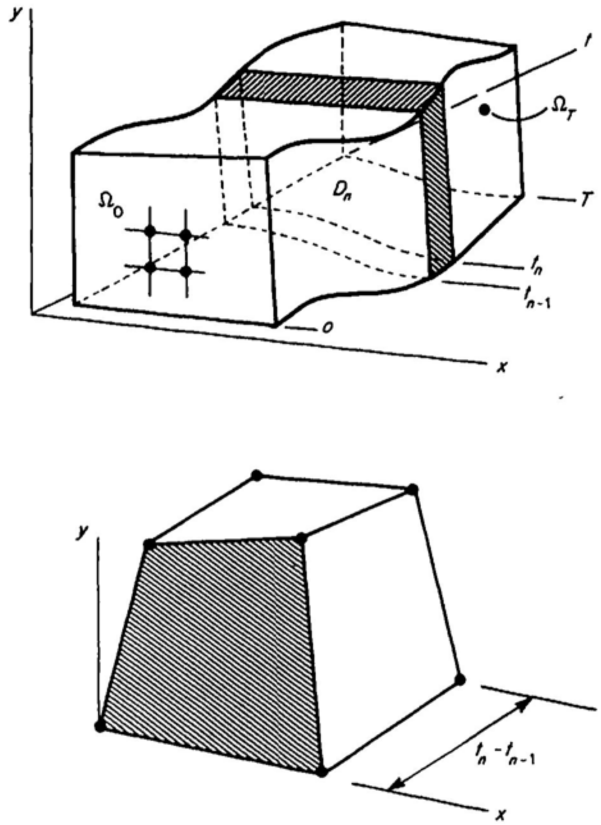

Figure 15.1 Space–time domain with strip D_n and a space–time finite element

boundary and initial conditions:

$$\left.\begin{aligned} \rho\left(\frac{\partial \mathbf{u}}{\partial t}+\mathbf{u}\cdot\nabla\mathbf{u}\right)-\mu\Delta\mathbf{u}+\nabla p=\mathbf{f} \\ \operatorname{div}\mathbf{u}=0 \end{aligned}\right\} \text{ in } D$$

with

$$\left.\begin{aligned} \mathbf{u}&=\mathbf{u}_0 \quad \text{on} \bigcup_t \Gamma_t^v, \\ \mathbf{t}(\mathbf{u},p)&=\mathbf{g} \quad \text{on} \bigcup_t \Gamma_t^T, \\ \mathbf{u}(0)&=\mathbf{U}_0 \quad (t=0), \end{aligned}\right\} \tag{15.1}$$

Here ρ is the mass density (a constant), $\mathbf{u}$ the flow velocity, μ the fluid viscosity, p the hydrostatic pressure, $\mathbf{f}$ the prescribed body force, $\mathbf{t}(\mathbf{u},p)$ is the traction on the boundary, $\mathbf{u}_0$ and $\mathbf{g}$ are prescribed boundary data and $\mathbf{U}_0$ is the prescribed initial velocity.

From many variational formulations which may be formulated for different purposes, we present here this one which laid down a foundation for computation. In the subsequent analysis we drop the nonlinear, convective term as well and assume that there exists at least one velocity field $\hat{\mathbf{u}}_0$ such that

$$\left.\begin{aligned} &\hat{\mathbf{u}}_0, \frac{\partial \hat{\mathbf{u}}_0}{\partial x_i}\in \mathbf{L}^2(D), \\ &\operatorname{div}\hat{\mathbf{u}}_0=0, \\ &\hat{\mathbf{u}}_0=\mathbf{u}_0 \quad \text{on} \bigcup_t \Gamma_t^v. \end{aligned}\right\} \tag{15.2}$$

Introducing the following spaces:

$$\mathbf{V}=\left\{\mathbf{v}=\mathbf{v}(\mathbf{x},t)\,|\,\mathbf{v}, \frac{\partial \mathbf{v}}{\partial x_i}\in\mathbf{L}^2(D), \quad \operatorname{div}\mathbf{v}=0, \quad \mathbf{v}=\mathbf{0} \quad \text{on} \bigcup_t \Gamma_t^v\right\},$$

$$\mathbf{H}=\left\{\boldsymbol{\phi}=\boldsymbol{\phi}(x,t)\,|\,\boldsymbol{\phi}\in\mathbf{H}^1(D), \quad \operatorname{div}\boldsymbol{\phi}=0, \quad \boldsymbol{\phi}=\mathbf{0} \quad \text{on} \bigcup_t \Gamma_t^v\right\} \tag{15.3}$$

and assuming that the solution $\mathbf{u}$ to equation (15.1) is sufficiently regular $(\partial\mathbf{u}/\partial t\in\mathbf{L}^2(D))$ the problem (15.1) may be characterized by the following variational statement. Find $\mathbf{u}$ such that

$$\mathbf{u}-\hat{\mathbf{u}}_0\in\mathbf{V} \quad \text{and} \quad A(\mathbf{u},\boldsymbol{\phi})=L(\boldsymbol{\phi}) \quad \forall\boldsymbol{\phi}\in\mathbf{H}. \tag{15.4}$$

In the above $A(\cdot,\cdot)$ and $L(\cdot)$ denote the bilinear and linear forms

$$\left.\begin{aligned} A(\mathbf{u},\boldsymbol{\phi})&=-\int_D \rho\mathbf{u}\cdot\frac{\partial\boldsymbol{\phi}}{\partial t}\,\mathrm{d}x\mathrm{d}t+\int_{\Omega_T}\mathbf{u}\cdot\boldsymbol{\phi}\,\mathrm{d}x+\mu\int_D (u_{i,j}+u_{j,i})\phi_{i,j}\,\mathrm{d}x\mathrm{d}t, \\ L(\boldsymbol{\phi})&=\int_D \mathbf{f}\cdot\boldsymbol{\phi}\,\mathrm{d}x\mathrm{d}t+\int_{\bigcup\Gamma_t^T}\mathbf{g}\cdot\boldsymbol{\phi}\,\mathrm{d}x\mathrm{d}t+\int_{\Omega_0}\mathbf{U}_0\boldsymbol{\phi}(0)\,\mathrm{d}x. \end{aligned}\right\} \tag{15.5}$$

One can prove that a solution to equation (15.4) exists and is unique.

For numerical purposes it is convenient to take into account the incompressibility condition by a penalty method. This leads to the new penalized variational formulation: Find u such that

$$\mathbf{u}-\hat{\mathbf{u}}_0\in \mathbf{V} \quad \text{and} \quad A(\mathbf{u}_\varepsilon, \boldsymbol{\phi}) + \frac{1}{\varepsilon}\int_D \operatorname{div} \mathbf{u}_\varepsilon \operatorname{div} \boldsymbol{\phi}\, d\mathbf{x}dt = L(\boldsymbol{\phi}) \quad \forall \boldsymbol{\phi}\in H \tag{15.6}$$

Here ε denotes the penalty parameter, and obviously the incompressibility condition has been dropped in both the definitions of V and H. Again one can prove that $\mathbf{u}_\varepsilon$ converges to u, when ε approaches 0.

The formulation (15.6) lays down the foundation for numerical purposes.

15.3 SPACE–TIME FINITE ELEMENTS

The idea of using finite element approximations in both space and time was introduced in the 1960s by Oden (1969) and has since been expanded and further developed by a number of authors. We mention in particular the work of Jamet (1978) which contains a priori error estimates of some interest with regard to the present study.

Our space–time discretization first involves a partition of the time interval into N-strips with endpoints t_i such that

$$0 = t_0 < t_1 < \cdots < t_N = T. \tag{15.7}$$

We denote

$$\Omega_n = \Omega_{t_n} \quad \text{and} \quad D_n = \bigcup_{t_{n-1}<t<t_n} \Omega_t,$$

and we shall apply the appropriate variational principle from the preceding section to each strip D_n. The initial data $\mathbf{U}_0$ shall apply to strip D_1 and the approximate solution calculated for each successive strip shall be used as initial data for the subsequent strip. Within each strip, Galerkin–finite element approximations are constructed. In the present study, we employ prismatic–triangular or prismatic–quadrilateral subparametric elements of the type indicated in Figure 15.1 over which the approximate solution is assumed to vary linearly in time, and for which hierarchical shape functions involving polynomials of degree 1, 2, or 3 are used in the spatial variables.

15.4 A POSTERIORI ERROR ESTIMATE

A key to meaningful adaptive finite element schemes is the availability of reliable estimates of the local error. While rigorous a posteriori error estimates are not available for many complex flow problems, it is possible to develop error estimators which provide information of sufficient accuracy to construct good adaptive schemes for many classes of practical problems.

Although our attention is focused primarily on the flow problem, for the sake of better understanding we present an estimate to a model heat-conduction problem with a varying domain, generalizing the results afterwards to the flow case. The numerical examples in the next section illustrate both cases.

15.4.1 A heat-conduction problem with moving boundaries

For the sake of simplicity we assume that the time-varying domain is polygonal at all times and that the approximations satisfy Dirichlet boundary conditions exactly.

The problem can be formulated as a sequence of variational problems defined on the strips D_n of the following form. Find

$$u \in H^1(D_n), \qquad u = u_0 \quad \text{on} \bigcup_{t_{n-1} < t < t_n} \Gamma_t^v, \tag{15.8}$$

such that

$$A(u, v) = L(v) \quad \forall v \in V_n,$$

where

$$V_n = \left\{ v \in H^1(D_n) | v = 0 \quad \text{on} \bigcup_{t_{n-1} < t < t_n} \Gamma_t^v \right\}, \tag{15.9}$$

$$A(u, v) = \int_{D_n} \left(-u \frac{\partial v}{\partial t} + \nabla u \cdot \nabla v \right) \mathrm{d}x\mathrm{d}t + \int_{\Omega_n} u \cdot v \, \mathrm{d}x, \tag{15.10}$$

$$L(v) = \int_{D_n} \mathrm{f} \cdot v \, \mathrm{d}x\mathrm{d}t + \int_{\bigcup \Gamma_t^T} g \cdot v \, \mathrm{d}s\,\mathrm{d}t + \int_{\Omega_{n-1}} uv \, \mathrm{d}x, \tag{15.11}$$

wherein $u|_{\Omega_{n-1}}$ is assumed to be known from information passed forward from the previous strip. In the above $u(x,t)$ is the temperature at the point x and time t, u_0, g is the prescribed boundary data, and f is the heat source intensity.

Consider a triangulation $\mathcal{T}_h$ of D_n over which piecewise polynomial shape functions of degree p in the spatial coordinates and linear in time are defined; these functions satisfying exactly the essential boundary conditions. We denote the subspace spanned by such functions as V_h^p, and the corresponding FE solution by u_h^p. We introduce also the error $e_h^p = u - u_h^p$ and the relative error of the first-order approximation with respect to the p-order as $e_h^{p,1} = u_h^p - u_h^1$.

It is easily verified that

$$A(u, v) = \int_{D_n} \left[\frac{\partial u}{\partial t} v + \nabla u \cdot \nabla v \right] \mathrm{d}x\mathrm{d}t + \int_{\Omega_{n-1}} u \cdot v \, \mathrm{d}x \tag{15.12}$$

and

$$A(u, u) = \int_{D_n} |\nabla u|^2 \, \mathrm{d}x\mathrm{d}t + \frac{1}{2} \int_{\Omega_n} u^2 \, \mathrm{d}x + \frac{1}{2} \int_{\Omega_{n-1}} u^2 \, \mathrm{d}x. \tag{15.13}$$

Thus it makes sense to define an energy norm by

$$\|u\|_A = [A(u,u)]^{1/2} \tag{15.14}$$

Obviously, we have

$$\|e_h^1\|_A \leqslant \|e_h^{p,1}\|_A + \|e_h^p\|_A. \tag{15.15}$$

Also

$$\|e_h^{p,1}\|_A^2 = A(\Pi e_h^{p,1}, e_h^{p,1} - v_h) \tag{15.16}$$

for $v_h \in V_h^1$ such that $v_h(\mathrm{x}^j) = e_h^{p,1}(\mathrm{x}^j)$ and

$$A(\Pi e_h^{p,1}, v_h) = \sum_{K\in\mathcal{T}_h} \int_K \nabla\psi_K \cdot \nabla v_h \,\mathrm{d}x + \int_{\Omega_{n-1}} e_h^{p,1} v_h \,\mathrm{d}x$$

$$+ \int_{D_n} \left[v_h \left(\frac{\partial u_h^p}{\partial t} - \frac{\partial u}{\partial t} \right) + \nabla e_h^p \cdot \nabla v_h \right] \mathrm{d}x\mathrm{d}t \quad \forall v_h \in V_h^{0p}. \tag{15.17}$$

Here, Π is a map from V_h^p onto V_h^{0p} defined so that

$$A(\Pi u_h, v_h) = A(u_h, v_h) \quad \forall u_h \in V_h^p, \quad \forall v_h \in V_h^{0p}, \tag{15.18}$$

$$V_h^{0p} = \{v_h \in V_h^p \mid v_h(\mathrm{x}^j) = 0\}. \tag{15.19}$$

Here, ψ_K = a solution of the local auxiliary problem

$$\int_K \nabla\psi_K \cdot \nabla v_h \,\mathrm{d}x\mathrm{d}t = \int_K r_h v_h \,\mathrm{d}x\mathrm{d}t + \hat{l}_K(v_h) \quad \forall v_h \in V_h^{0p}(K) \tag{15.20}$$

$$r_h = f + \Delta u_h^1 - \frac{\partial u_h^1}{\partial t} \tag{15.21}$$

$$\hat{l}_K(v_h) = \int_{\partial K - \Gamma} -\frac{1}{2}\left(\frac{\partial u_h^1}{\partial n} + \frac{\partial u_h^{1*}}{\partial n^*} \right) v_h \,\mathrm{d}s + \int_{\partial K \cap \Gamma} \left(g - \frac{\partial u_h^1}{\partial n} \right) v_h \,\mathrm{d}s \tag{15.22}$$

where $n^* = -n$ and u_h^{1*} denotes the approximate solution for the adjacent element.

It is possible to prove that constants C_1 and C_2 exist such that

$$\int_{D_n} |\nabla w_h|^2 \,\mathrm{d}x\mathrm{d}t \leqslant C_1 \int_{D_n} |\nabla e_h^{p,1}|^2 \,\mathrm{d}x\mathrm{d}t, \tag{15.23}$$

$$\int_{\Omega_{n-1}} |w_h|^2 \,\mathrm{d}x \leqslant C_2 \int_{\Omega_{n-1}} |e_h^{p,1}|^2 \,\mathrm{d}x \tag{15.24}$$

for $w_h = e_h^{p,1} - \hat{v}_h$, where $\hat{v}_h(\mathrm{x}^j) = e_h^{p,1}(\mathrm{x}^j)$, and we assume that $C_3 > 0$ exists such that the last two terms in equation (15.19) are bounded by $C_3[\int_{D_n} |\nabla e_h^{p,1}|^2 \,\mathrm{d}x\mathrm{d}t]^{1/2}$.

These considerations lead to the bound

$$\| e_h^{p,1} \|_{A'}^2 \leqslant \left\{ C_1 \left(\sum_{K \in \mathcal{T}_h} |\psi_K|^2 \right)^{1/2} + C_3 \right\} |e_h^{p,1}|_{1,D_n} + \{C_2 - \tfrac{1}{2}\} \| e_h^{p,1} \|_{L^2(\Omega_{n-1})}^2, \tag{15.25}$$

wherein ψ_K is defined by equation (15.19),

$$\| u \|_{A'}^2 \overset{\text{def}}{=} \int_{D_n} |\nabla u|^2 \, dx dt + \frac{1}{2} \int_{\Omega_n} |u|^2 \, dx, \tag{15.26}$$

$$|e_h^{p,1}|_{1,D_n}^2 = \int_{D_n} |\nabla e_h^{p,1}|^2 \, dx dt. \tag{15.27}$$

Observing that for real numbers $a, b, c, d > 0$,

$$\tfrac{1}{2}a^2 + d^2 \leqslant bd + \tfrac{1}{2}c^2 \rightarrow [\tfrac{1}{2}a^2 + d^2]^{1/2} \leqslant b + 2^{-1/2}c$$

we reduce equation (15.24) further to

$$\| e_h^1 \|_{A'} \leqslant C_1 \left(\sum_{K \in \mathcal{T}_h} |\psi_K|^2 \right)^{1/2} + \sqrt{C_2 - \tfrac{1}{2}} \| e_h^1 \|_{L^2(\Omega_{n-1})} + E, \tag{15.28}$$

where

$$E = C_3 + \sqrt{C_2 - \tfrac{1}{2}} \| e_h^p \|_{L^2(\Omega_{n-1})} + \| e_h^p \|_{A'}. \tag{15.29}$$

When the solution u is sufficiently smooth, and the mesh sufficiently refined, we expect the quantity E to be negligible in comparison with the term involving ψ_K.

15.4.2 Flow problem

The extension of the methodology outlined in Section 15.4.1 to the general viscous flow problem described earlier is straightforward and very similar to that used for problem (15.8). We must note that the unknown velocity field $\mathbf{u}$ is vector-valued and that the bilinear form $\int_{D_n} \nabla u \cdot \nabla v \, dx dt$ should be replaced by the virtual work

$$G(\mathbf{u}, \mathbf{v}) = \mu \int_{D_n} (u_{i,j} + u_{j,i}) v_{i,j} \, dx dt + \varepsilon^{-1} \int_{D_n} \operatorname{div} \mathbf{u} \operatorname{div} \mathbf{v} \, dx dt, \tag{15.30}$$

etc. Using assumptions completely analogous to those used in deriving equation (15.28), we obtain the estimate

$$\begin{aligned} \| \mathbf{e}_h^1 \|_G &\equiv \left[G(\mathbf{e}_h^1, \mathbf{e}_h^1) + \frac{1}{2} \int_{\Omega_{n-1}} |\mathbf{e}_h^1|^2 \, dx \right]^{1/2} \\ &\leqslant C_1 \left\{ \sum_{K \in \mathcal{T}_h} |\psi_K|_K^2 \right\}^{1/2} + \sqrt{C_2 - \tfrac{1}{2}} \int_{\Omega_{n-1}} |\mathbf{e}_h^1|^2 \, dx, \end{aligned} \tag{15.31}$$

where

$$|\psi_K|_K^2 = \int_K [\mu(\psi_{Ki,j} + \psi_{Kj,i})\psi_{Ki,j} + \varepsilon^{-1}(\operatorname{div}\psi_K)^2]\,\mathrm{d}x\mathrm{d}t \tag{15.32}$$

and ψ_K is the solution to the local auxiliary problem

$$\psi_K \in \mathbf{V}_h^{0p}(K)$$

$$G_K(\psi_K, \mathbf{w}_h) = \int_K \left[f_i - \left(\frac{\partial u_{hi}^1}{\partial t} - \sigma_{ij}(\mathbf{u}_h^1)_{,j} \right) \right] w_{hi}\,\mathrm{d}x\mathrm{d}t - \int_{\partial K - \Gamma} \bar{\mathbf{t}}(u_h^1)\cdot \mathbf{w}_h\,\mathrm{d}s\mathrm{d}t$$

$$+ \int_{\partial K \cap \Gamma^T} (\mathbf{g} - \mathbf{t}(\mathbf{u}_h^1))\cdot \mathbf{w}_h\,\mathrm{d}s\mathrm{d}t \quad \forall \mathbf{w}_h \in \mathbf{V}_h^{0p}(K). \tag{15.33}$$

Here $G_K(\cdot,\cdot)$ is the restriction of $G(\cdot,\cdot)$ to element $K, \sigma_{ij}(\mathbf{u}) = \mu(u_{i,j} + u_{j,i}) + \varepsilon^{-1}\operatorname{div}\mathbf{u}\delta_{ij}$, and $\bar{\mathbf{t}}$ is the difference of tractions on an element side.

In the above bound, the constant C_2 is the same as that in Section 15.4.1, whereas C_1 is not since the 'energy norm' has now changed. In particular, C_1 is now derived from the condition that

$$G(\mathbf{u}_h - \hat{\mathbf{v}}_h, \mathbf{u}_h - \hat{\mathbf{v}}_h) \leqslant C_1^2 G(\mathbf{u}_h, \mathbf{u}_h) \quad \forall \mathbf{u}_h \in \mathbf{V}_h^p$$

where $\hat{\mathbf{v}}_h$ is the first-order (linear) basis function interpolating $\mathbf{u}_h$ exactly at the nodes (triangular vertices).

15.5 NUMERICAL RESULTS

We conclude this chapter with a series of numerical experiments concerning both the flow, as well as our model (heat-conduction) problems.

15.5.1 Mesh enrichment strategy

Although the *a posteriori* error estimate prescribed in the previous section is of a global time, i.e. estimates the global-integral type error over the whole domain, we make use of it in a local manner. More precisely, if η_K denotes the normalized contribution of the element K to the estimate, the new variable order of approximation is defined in the following way:

(a) For triangular elements
  - $0 \leqslant \eta_K < \delta_1$ first-order approximation
  - $\delta_1 \leqslant \eta_K < \delta_2$ second-order approximation
  - $\delta_2 \leqslant \eta_K \leqslant 1$ third-order approximation

(b) For quadrilaterals
  - $0 \leqslant \eta_K < \delta$ first-order approximation
  - $\delta \leqslant \eta_K \leqslant 1$ second-order approximation

At this stage, the numbers $\delta_1, \delta_2, \delta$ are chosen intuitively and this part of the work requires some further research. We will specify $\delta_1, \delta_2, \delta$ separately for each of the examples.

15.5.2 Investigation of local and global behavior of the a posteriori error estimate

The *a posteriori* error estimate has been tested on the following example.

Let $\Omega = (0, 4) \times (0, 3)$ (fixed domain). The purely Dirichlet boundary and initial data as well as the right-hand side of the equation correspond to the following (exact) solution:

$$u = 10\,e^{-5(x-1)^2} x(4-x)y(3-y)t,$$

where u exhibits some kind of 'singular' behavior for $x = 1$. All the comparison has been made on the base of one time-step solution $\Delta t = 1$. Because of linear dependence of u on t the error is due to the space approximation only. (In the sense that for an exact space approximation, the error would be equal to zero.)

The approximate mesh presented in Figure 15.2. consists of 24 prismatic triangular elements. The problem has been solved three times:

(1) with the first-order approximation (12 freedom degrees);

(2) with variable-order approximation (68 freedom degrees) (refined mesh, see Figure 15.2);

(3) with the third-order approximation (176 freedom degrees).

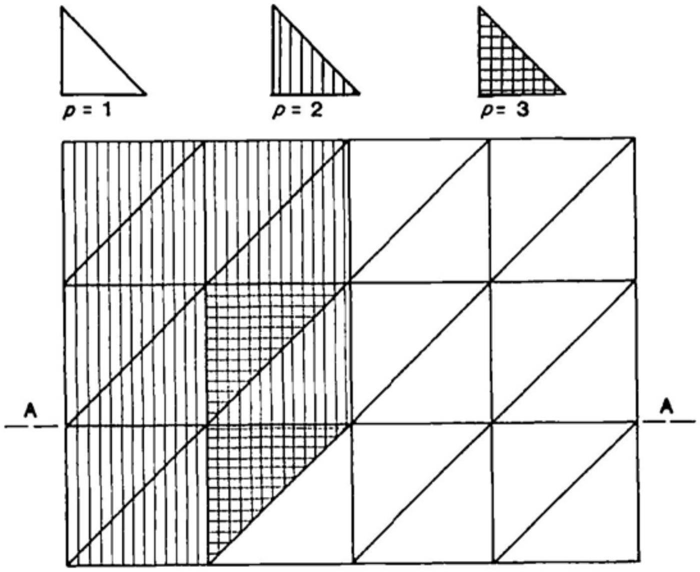

Figure 15.2 Mesh for the first problem. Local order of approximation for the refined mesh

Table 15.1 Element Contributions to the Error

Element K no.	Error for first order approximation (12 degrees of freedom) $\int_K \nabla e^2$	$\frac{1}{2}\int_{K\cap\Omega_1} e^2$	Error for first mesh refinement (68 degrees of freedom) $\int_K \nabla e^2$	$\frac{1}{2}\int_{K\cap\Omega_1} e^2$	Error for second mesh refinement (176 degrees of freedom) $\int_K \nabla e^2$	$\frac{1}{2}\int_{K\cap\Omega_1} e^2$
1	351.25	240.92	42.46	0.80	43.22	0.82
2	357.20	23.30	362.79	72.45	36.18	1.28
3	684.47	797.34	193.67	5.06	122.08	2.48
4	571.99	37.96	258.20	77.40	49.62	1.43
5	591.92	257.68	620.21	51.92	57.97	1.17
6	116.53	6.54	114.57	3.70	7.88	0.12
7	308.51	30.07	4.73	0.12	3.95	0.06
8	1065.99	341.39	45.82	1.34	42.55	1.15
9	1310.53	174.41	83.07	1.43	80.90	1.66
10	1420.99	933.72	125.12	2.81	103.09	2.75
11	831.91	107.03	77.82	1.10	74.36	1.81
12	542.58	264.43	288.54	28.39	68.81	1.42
13	0.00	0.00	0.00	0.00	0.00	0.00
14	0.64	0.01	0.40	0.01	0.08	0.00
15	0.00	0.00	0.00	0.01	0.06	0.00
16	2.04	0.06	0.29	0.11	0.50	0.01
17	0.00	0.00	0.00	0.08	0.18	0.01
18	0.64	0.01	0.40	0.17	0.27	0.01
19	0.00	0.00	0.00	0.00	0.00	0.00
20	0.00	0.00	0.00	0.00	0.00	0.00
21	0.00	0.00	0.00	0.00	0.00	0.00
22	0.00	0.00	0.00	0.00	0.00	0.00
23	0.00	0.00	0.00	0.00	0.00	0.00
24	0.00	0.00	0.00	0.00	0.00	0.00
Total	8157.25	1607.47	2218.16	123.48	691.76	8.12

The respective values of the constants δ_1 and δ_2 are: $\delta_1 = 1/9$; $\delta_2 = 4/9$.

Let us recall that the error is measured in the following energy norm:

$$\|e\|_E^2 = \int_D |\nabla e|^2 \, dx dt + \frac{1}{2}\int_{\Omega_1} e^2 \, dx. \tag{15.34}$$

Table 15.1 presents the contribution of each element to the error for all three approximate solutions.

Finally, Table 15.2 shows the contribution of each element to the a posteriori error estimate compared with the contribution of the first-order approximation error itself. Similar, although obviously not identical behavior is observed. Also, one can see that the contribution of the error due to initial data is of one, two orders less than that from the error indicator function and therefore may be neglected.

Table 15.2 Element Contributions to the *a posteriori* Error Estimate

			Error estimate for the first order approx. soln.		
				Normalized	
Element K no.	First-order appr. error	Normalized error	$\int_K \nabla\phi_K^2$	$\int_K \nabla\phi_K^2$	$\int_{K\cap\Omega_0} e^2$
1	592.17	0.25	71.01	0.03	1.70
2	380.50	0.16	411.16	0.18	1.70
3	1481.81	0.63	221.64	0.10	5.09
4	609.95	0.26	508.68	0.23	1.69
5	849.60	0.36	257.75	0.12	1.69
6	123.07	0.05	22.73	0.01	0.00
7	338.58	0.14	17.30	0.01	1.13
8	1407.38	0.60	1177.28	0.53	4.22
9	1484.94	0.63	463.03	0.21	8.12
10	2354.71	1.00	2239.35	1.00	9.26
11	938.94	0.40	418.34	0.19	4.39
12	807.01	0.34	348.68	0.16	1.69
13	0.00	0.00	5.95	0.00	0.11
14	0.65	0.00	7.39	0.00	1.61
15	0.00	0.00	7.81	0.00	2.30
16	2.10	0.00	72.68	0.03	4.55
17	0.00	0.00	42.06	0.02	1.82
18	0.65	0.00	68.43	0.03	1.25
19	0.00	0.00	0.00	0.00	0.00
20	0.00	0.00	1.45	0.00	0.11
21	0.00	0.00	0.28	0.00	0.11
22	0.00	0.00	0.76	0.00	0.40
23	0.00	0.00	0.95	0.00	0.14
24	0.00	0.00	2.26	0.00	0.14
Total	9764.72		6367.08		53.35

Finally, we can estimate the global quality of the error estimate. Since all the elements are identical with the master element, we can assume C_1, C_2 equal to those for the master element, which can be proved to be equal:

$$C_1 = \sqrt{3}, \qquad C_2 = 4$$

thus, the ratio of effectiveness defined as

$$r = \frac{\text{error estimate} - \text{error}}{\text{norm of the solution}}$$

is equal to

$$r = \frac{166.96 - 98.82}{105.46} = 0.646.$$

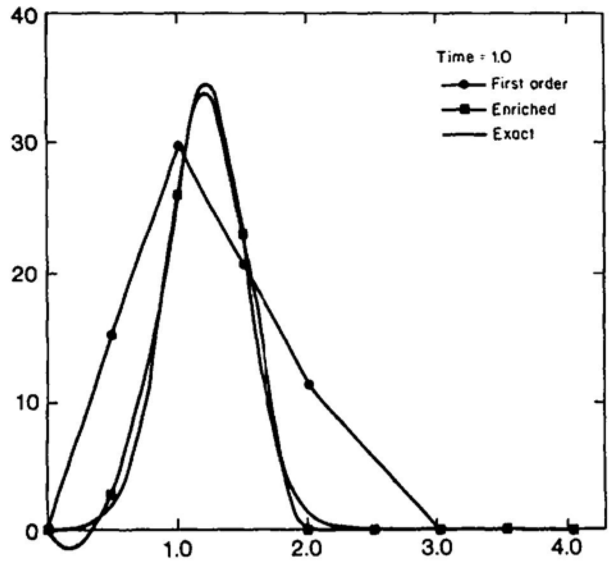

Figure 15.3 Heat conduction problem. Computed solutions on section AA for $p = 1$ and adaptive correction for time $t = 1.0$

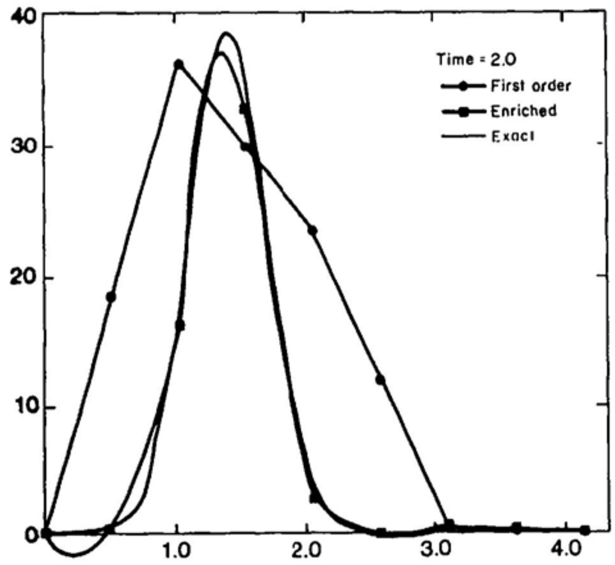

Figure 15.4 Heat conduction problem. Computed solutions on section AA for $p = 1$ and adaptive correction for time $t = 2.0$

15.5.3 Solution of the heat-conduction problem in a moving domain

Let $\Omega_t = (0, 4 + 0.1t) \times (0.3)$. The purely Dirichlet boundary and initial data, as well as the right-hand side of the equation correspond to the following exact solution:

$$u = 10\,e^{-5(x-1-0.2t)^2} x(4 + 0.1t - x)y(3 - y) \cdot C,$$

where

$$C = \begin{cases} t & \text{for} \quad 0 < t < 0.5, \\ 1 & \text{for} \quad t > 0.5. \end{cases}$$

The problem has been solved for the mesh (see Figure 15.2) with 24 elements. The time-step has been chosen as $\Delta t = 0.1$. The first 20 time-steps have been calculated. The constants δ_1 and δ_2 have been chosen as $\delta_1 = 1/20$, $\delta_2 = 1/2$.

Figures 15.3 and 15.4 present the computed first-order and enriched solutions on the section AA (see Figure 15.2) with comparison to the exact solution.

15.5.4 Flow problem in a moving domain

As the final example, we have chosen a 'Poiseuille-type' flow through the duct with decreasing cross-section. At time $t = 0$, the spatial domain corresponds to $\Omega_0 = (0, 12) \times (0, 10)$ and is discretized using a 6×5 mesh as in the previous

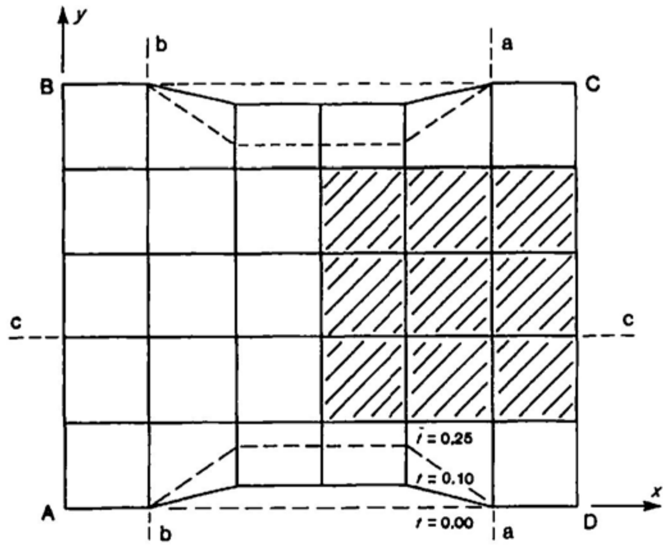

Figure 15.5 Flow problem in moving domain. Mesh enrichment for $t = 0.10$ and $t = 0.25$

example. For $t > 0$ the lateral boundaries in the central portion of the duct move into the duct with a constant speed equal to 5, as shown in Figure 15.5. Kinematic boundary conditions are prescribed along parts AB, BC, DA of the duct boundary, while the tractions are prescribed on CD. The 'nonslip' boundary condition, applied on the portions BC and DA of the boundary implies that the velocity of the fluid there coincides with the velocity of the boundary. The applied velocities on AB, the applied tractions on CD, the initial conditions, and the body force were chosen to correspond to steady-state Poiseuille flow in an infinite duct. This is intended to model the transient local disturbance of a Poiseuille flow induced by local contraction of the cross-section of the duct.

The problem has been solved with a mesh that remains fixed in the interior of the domain but deforms to follow the motion of the boundary on BC and DA, as shown in Figure 15.5. The velocity components for the steady-state Poiseuille flow are

$$u = y(10 - y), \qquad v = 0$$

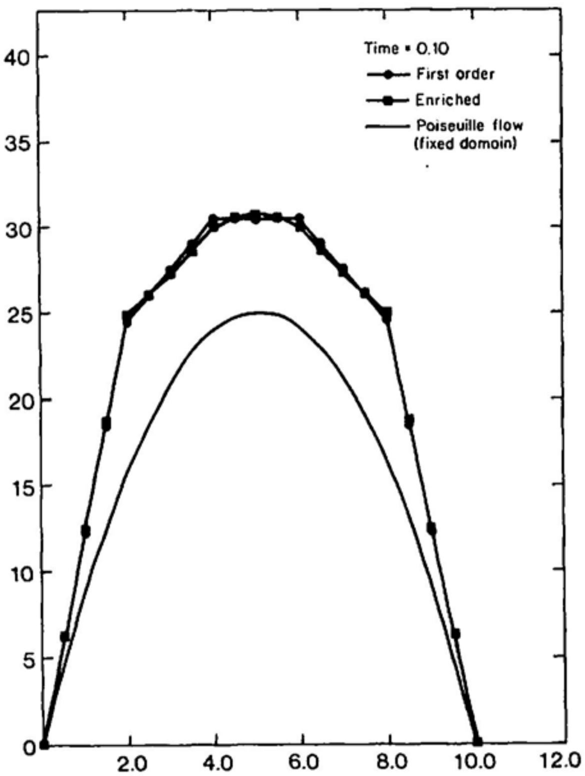

Figure 15.6 Flow problem in moving domain. Computed solutions on section aa for time $t = 0.10$

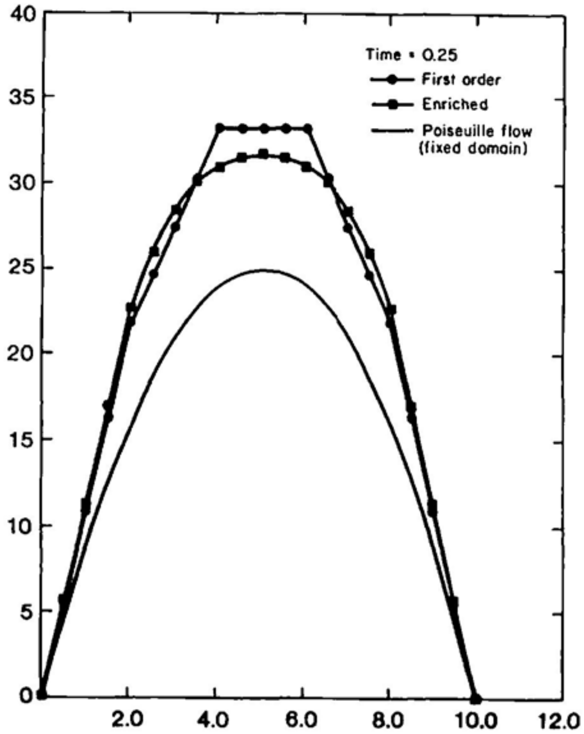

Figure 15.7 Flow problem in moving domain. Computed solutions on section aa for time $t = 0.25$

and the corresponding body force

$$f_x = 2, \qquad f_y = 0$$

and the pressure is given by $p = 0$.

The parameters used for the solution are: time-step = 0.05; penalty parameter $\varepsilon = 10^5$; coefficient $\delta = 0.25$.

Figure 15.5 shows the mesh enrichment at times $t = 0.10$, 0.25 (the mesh was the same). Figures 15.6 and 15.7 present the computed velocity profiles for the u-components of the fluid velocity along sections a–a.

REFERENCES

Demkowicz, L., Oden, J. T., and Strouboulis, T. (1984), 'Adaptive finite elements for flow problems with moving boundaries. I. Variational principles and a posteriori estimates', *Comp. Meth. Appl. Mech. Eng.*, **46**(2), 217–251.

Jamet; P. (1978), 'Galerkin-type approximations which are discontinuous in time for parabolic equations in a variable domain', *SIAM J. Numer. Anal.*, **15**(5), 912–928.

Oden, J. T. (1969), 'A general theory of finite elements. I. Applications', *Int. J. Num. Meth. Eng.*, 1, 247–259.